Genes & Diseases (2023) 10, 1175–1179

Available online at www.sciencedirect.com

ScienceDirect

journal homepage: www.keaipublishing.com/en/journals/genes-diseases

RAPID COMMUNICATION

Bone Morphogenic Protein 9 (BMP9)/ Growth Differentiation Factor 2 (GDF2) modulates mouse adult hippocampal neurogenesis by regulating the survival of early neural progenitors

Adult neurogenesis occurs in two specialized regions of the mammalian brain, the subventricular zone (SVZ) and the subgranular zone (SGZ) of the dentate gyrus (DG).[1] Adult hippocampal neural stem cells (NSCs), referred to as Type 1 cells represented by radial glia-like cells (RGLs), generate Type 2 cells that are divided into Type 2a and Type 2 b subpopulations, the latter of which give rise to Type 3 cells (neuroblasts). Type 3 cells exit the cell cycle and give rise to immature neurons that subsequently mature into functional granule cells (Fig. 1A). The neural regenerative capacity depends on maintaining a reservoir of NSCs and the integrity of the neurogenic niche, which are regulated by neurotransmitters and numerous signals including Notch, Wnt, and BMPs.[1] Here we showed that BMP9 (a.k.a., GDF2) deficiency altered the dynamics of adult hippocampal neurogenesis as proliferative activity was decreased in Type 2a cells in *Bmp 9* knockout (*Bmp9*KO) mice (Fig. S1). Surprisingly, the number of cells committed to the neuronal lineage was comparable to wildtype while the label retention was increased in immature neurons, suggesting mitigation of reduced proliferation in *Bmp9*KO mice by increased cell survival. We also found *Bmp9* was not expressed in the adult brain, precluding cell-autonomous regulation of neurogenic populations like other BMPs. Our findings thus demonstrate BMP9 regulates adult homeostatic neurogenesis.

We previously identified BMP9 as one of the most potent osteogenic BMPs.[2] Emerging evidence indicates BMP9 exerts diverse functions in glucose metabolism, angiogenesis, stem cell differentiation and maintenance of basal forebrain cholinergic neurons (BFCN)[2;].[3] However, whether endogenous BMP9 is necessary for adult neurogenesis has not been fully studied. We generated global *Bmp 9* knockout (*Bmp9KO*) mice (Fig. S1A, B).[4] Using this model, we first tested whether BMP9 deficiency affected proliferation in the SGZ. To detect subtype specific changes, we pulsed the mitotic cells with CldU in both wildtype and *Bmp9*KO mice, and combined immunostaining for CldU with lineage specific markers such as GFAP, SOX2, DCX and NeuN (Fig. S2A, B). The design-based stereology changes were used to achieve the resolution of detecting such differences and quantitative estimates with high precision. Based on pilot studies, we used 50% sampling coverage and obtained CE < 1.2 for all BrdU $^{+}$ cell counts.

Since Type 1 cells are heterogeneous with different capacities for self-renewal and generating neurogenic and gliogenic progeny, we quantified astrocytes based on morphology and expression of GFAP and SOX2 to evaluate the BMP9 effect on Type 1 cell fate potential (Fig. 1B, *a* & *d*). The median number of astrocytes for wildtype mice and *Bmp9*KO mice groups did not differ (Fig. 1B, *d*), indicating the reduction in Type 2a cell proliferation in *Bmp9*KO mice was not at the cost of astrocyte differentiation. Within the total SOX2^{+} population, the proportions of Type 1 cells, Type 2 cells, and astrocytes were not different between wildtype and *Bmp9*KO mice (Fig. 1B, *e*).

Using GFAP and SOX2 as markers to distinguish Type 1 (GFAP^{+}/SOX2^{+}) from Type 2a (GFAP^{-}/SOX2^{+}) cells, we first evaluated the effect of BMP9 deficiency on the proliferative activity of early precursors (Fig. 1C, *a-e*). Whereas Type 1 cells in wildtype and *Bmp9*KO groups did not differ significantly (Fig. 1C, panel *b*), there were significantly fewer proliferating Type 2a cells (BrdU^{+}/GFAP^{-}/SOX2^{+}) for

Peer review under responsibility of Chongqing Medical University.

https://doi.org/10.1016/j.gendis.2023.02.018

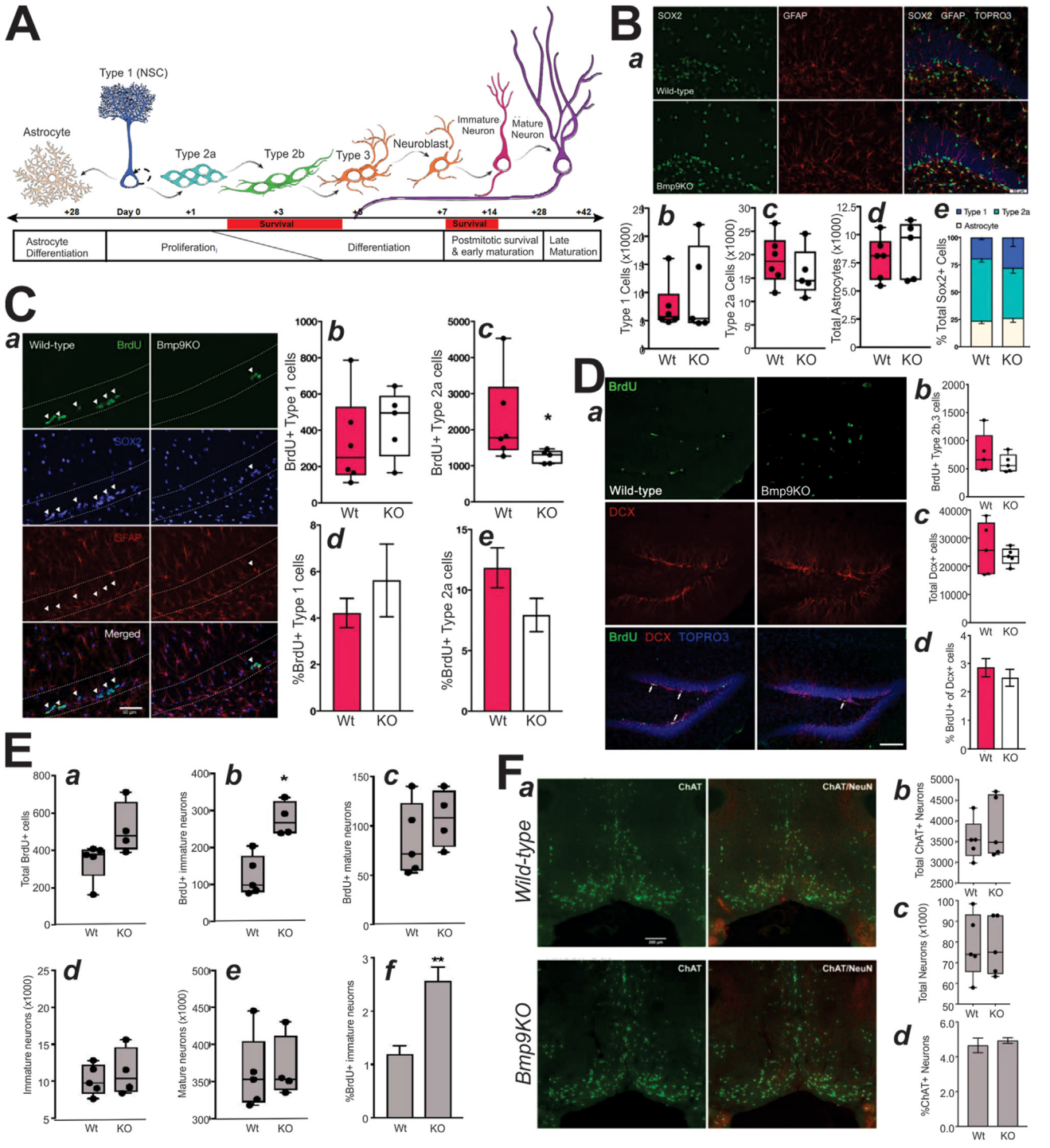

Figure 1 BMP9 regulates neurogenesis in mouse adult hippocampus. **(A)** Lineage progression and timeline of neural development in the adult hippocampus. Type 1 cells are multipotent neural stem cells (NSCs) that develop into new neurons and astrocytes in the SGZ. Through asymmetric division, Type 1 cells both self-renew and produce an intermediate progenitor cell. Within the neurogenic lineage, there are three types of intermediate progenitor cells (IPCs). These populations undergo progressive rounds of symmetric cell division and differentiation to amplify the neural precursor population. Most of these cells undergo apoptosis. Progenitor cells that survive complete differentiation within one week. Over the following three weeks new-born cells acquire morphological features of mature neurons. Neurogenic output is dependent on combinatorial regulation of progenitor proliferation, differentiation, survival, and maturation. Continual generation of new neurons throughout life is associated with maintenance of the NSC pool. The production of new astrocytes similarly depends on Type 1 NSCs. Following cell-cycle exit, post-mitotic Type 1 cells differentiate into astrocyte progenitors. In contrast to IPCs of the neurogenic lineage, astrocyte progeni-tors have restricted proliferation. Similar to IPCs, astrocytes progenitors are successfully differentiated into astrocytes within one week and reach maturation by 4 weeks. **(B)** *Bmp9*KO mice do not have an altered distribution of early precursors and astrocytes. **(*a*)** Coronal

*Bmp9*KO than for wildtype mice (Fig. 1C, *c*), suggesting that BMP9 deficiency may reduce proliferation of Type 2a progenitors.

To determine whether *Bmp9*KO mice had fewer proliferating Type 2a cells due to a smaller Type 2a population and/or reduced proliferative activity within the population, we analyzed the percentage of labeled Type 2a cells ($BrdU^+/GFAP^-/SOX2^+$) within the total Type 2a cell population ($GFAP^-/SOX2^+$) for each group. *Bmp9*KO mice demonstrated a notable, but not significant, reduction in proliferative activity relative to wild-type mice (Fig. 1C, *e*), while the total Type 2a cell population for wildtype and *Bmp9*KO groups did not differ significantly (Fig. 1B, *c*). There was no significant difference in the percentage of S-labeled in the Type 1 population either (Fig. 1C, *d*), while the total Type 1 cell population for wildtype and *Bmp9*KO mice did not differ (Fig. 1B, *b*). These data indicate the decreased Type 2a population in *Bmp9*KO mice was not caused by aberrant Type 1 activation and consequent depletion of the Type 1 population.

As angiogenesis and neurogenesis are closely associated, we quantified the endothelial cell progenitor-containing proportion of unidentified $BrdU^+$ cells ($BrdU^+/SOX2^-/GFAP^-$). We found the proportion of $BrdU^+/SOX2^-/GFAP^-$ cells was not different between wildtype and *Bmp9*KO (Fig. S3A), indicating endothelial cell hypersprouting was not present in *Bmp9*KO mice. CD31 immunostaining did not reveal vasculature structural alterations in *Bmp9*KO mice

sections were immunostained with SOX2 and GFAP to identify astrocytes (SOX2+/GFAP+), Type 1 cells (SOX2+/GFAP+), and Type 2a cells (SOX+/GFAP-). Astrocytes and Type 1 cells were differentiated by morphological characteristics. Note the apical processes crossing the granule cell layer, which is defined by the nuclear counterstain TOPRO3 in the merged panel of the representative image. **(*b-e*)** Quantitative analysis using design-based stereology showed the number the total number of (*b*) Type 1 cells, (*c*) Type 2a cells, and (*d*) astrocytes in wild-type and *Bmp9*KO mice does not differ. (*e*) The relative proportions of Type 1 cells, Type 2a cells, and astrocytes within the total SOX2+ population is not significantly different between wild-type and *Bmp9*KO mice. Scale bar equals 50 μm. Whiskers on boxplots represent maximum and minimum values and points represent values for individual mice. $n = 6$ for wild-type mice; $n = 5$ for *Bmp9*KO mice. Error bars on bar charts represent ± SEM for each group. **(C)** Proliferation of early progenitors is reduced in *Bmp9*KO mice. **(*a*)** Three month old male wild-type and *Bmp9*KO mice were injected with CldU to label cells in S-phase according to the experimental paradigm in Figure S1. Coronal sections were immunostained with BrdU, SOX2, and GFAP to identify proliferating Type 1 cells (BrdU+/SOX2+/GFAP+) and proliferating Type 2a cells (BrdU+/SOX+/GFAP-). Dashed lines delineate the SGZ, arrowheads show clusters of BrdU + cells in each panel. Note BrdU + cells primarily colocalize with SOX2 in both groups and that *Bmp9*KO mice have fewer BrdU + cells. **(*b*)** Quantitative analysis using design-based stereology showed the number of BrdU + Type 1 cells is not different between wild-type and *Bmp9*KO mice, but **(*c*)** significantly fewer BrdU + Type 2a cells in *Bmp9*KO mice. **(*d*)** The proportion of BrdU + Type 1 cells and **(*e*)** BrdU + Type 2a cells does not differ significantly between wild-type and*Bmp9*KO mice. Scale bar equals 50 μm. Whiskers on boxplots represent maximum and minimum values and points represent values for individual mice. $n = 6$ for wild-type mice; $n = 5$ for *Bmp*9KO mice. Error bars on bar charts represent ±SEM for each group. $^*P < 0.05$. **(D)** Deregulation of neural precursors does not decrease the success of neuronal lineage commitment in *Bmp9*KO mice. **(*a*)** Three month old male wild-type and *Bmp*9KO mice were injected with CldU to label cells in S-phase according to the experimental paradigm in Figure A.2. Coronal sections were immunostained with BrdU and DCX to identify proliferating Type 2b/3 cells (BrdU+/DCX+). Note colocalization of BrdU and DCX is limited in both animals and that *Bmp9*KO mice have fewer BrdU + cells in the representative image. **(*b-d*)** Quantitative analysis using design based stereology showed the number of (*b*) BrdU + Type 2b/3 and (*c*) total number of DCX + cells is not different between wild-type and *Bmp9*KO mice. (*d*) The relative proportion of BrdU + Type 2b/3 to all cells committed to the neurogenic lineage is not different between wild-type and *Bmp9*KO groups. Scale bar equals 50 μm. Whiskers on boxplots represent maximum and minimum values and points represent values for individual mice. $n = 6$ for wild-type mice; $n = 5$ for *Bmp*9KO mice. Error bars on bar charts represent ± SEM for each group. **(E)** Survival of new-born neurons is increased in *Bmp9*KO mice. **(*a-f*)** Three month old male wild-type and *Bmp*9KO mice were injected with CldU to label cells in S-phase according to the experimental paradigm in Figure A.2 B. Coronal sections were immunostained for BrdU, DCX, and NeuN to evaluate survival after 23 days on the basis of label retention. Quantitative analysis using design based stereology showed **(*a*)** a marked increase in the number of label-retaining cells (BrdU+) in *Bmp9*KO mice. The total number of label-retaining cells is increased in *Bmp9*KO mice. **(*b*)** The number of label-retaining immature neurons in *Bmp9*KO mice is significantly greater than wild-type mice, but **(*c*)** the number of label-retaining mature neurons does not differ between the two groups. **(*d*)** The total number of immature neurons and **(*e*)** mature neurons is not significantly different between wild-type and *Bmp9*KO mice. **(*f*)** The percentage of label-retaining immature neurons is significantly greater in *Bmp9*KO mice. Whiskers on boxplots represent maximum and minimum values and points represent values for individual mice. $n = 5$ for wild-type mice; $n = 4$ for *Bmp*9KO mice. Error bars on bar charts represent ± SEM for each group. $^*P < 0.05$, $^{**}P < 0.01$. **(F)** Endogenous BMP9 is not necessary for cholinergic support in the medial septum and diagonal band of Broca. **(*a*)** Coronal sections from the medial septum and vertical diagonal Band of Broca were immunostained for ChAT and NeuN to identify the cholinergic neurons and neurons irrespective of phenotype. **(*b-d*)** Quantitative analysis using design-based stereology showed (*b*) the number of cholinergic (ChAT+) neurons in basal forebrain structures do not differ between wild-type and *Bmp9KO* mice. (*c*) The total number of neurons, irrespective of phenotype does not differ between wild-type and *Bmp9KO* mice. (*d*) There is no difference between the percentage of ChAT positive neurons with respect to the entire neuronal population between wild-type and *Bmp9KO* mice. Scale bar equals 200 μm Whiskers on boxplots represent maximum and minimum values and points represent values for individual mice. $n = 5$ for wild-type mice; $n = 5$ for *Bmp*9KO mice. Error bars on bar charts represent ± SEM for each group. Whiskers on boxplots represent maximum and minimum values. Error bars on charts represent ± SEM for each group.

(Fig. S3B). These data suggest dysregulated Type 2a cells in *Bmp9*KO mice may be not related to aberrant angiogenesis.

Since the Type 2a to Type 2 b transition is marked by SOX2 suppression and DCX upregulation, we evaluated BMP9-null effect on the total number of proliferating Type 2 b progenitors ($BrdU^+/DCX^+$) (Fig. 1D, *b*), the total number of DCX^+ cells (Fig. 1D, *c*), and the percentage of proliferating Type 2b/3 in the total DCX^+ population (Fig. 1D, *d*). Small, but statistically non-significant reductions were observed in *Bmp9*KO mice for all three measurements. BMP9 deficiency therefore may not significantly alter Type 2b/3 proliferation and the number of Type 2a cells committed to neurogenic lineage. Thus, BMP9 deficiency does not alter neuronal lineage commitment.

To investigate whether BMP9 deficiency affected survival of postmitotic cells, we used CldU pulse-labeling to birthdate cells prior to cell cycle exit (Fig. S2B), and found *Bmp9*KO mice had more label-retaining-cells (LRCs; $BrdU^+/DCX^+/NeuN^+$) after 23 days (Fig. 1E, *a*). Using DCX and NeuN staining, we found *Bmp9*KO mice had a significantly greater number of LRCs (Fig. 1E, *b*), without change in the total number of LRCs (Fig. 1E, *c*). We quantified the total number of cells in each of these population, and found no difference in either the total population of immature ($DCX^+/NeuN^+$) (Fig. 1E, *d*) or mature neurons ($DCX^-/NeuN^+$) (Fig. 1E, *e*) between wildtype and *Bmp9*KO mice. We further found *Bmp9*KO mice had a significantly greater percentage of LRC immature neurons relative to wildtype (Fig. 1E, *f*). Thus, BMP9 deficiency may enhance immature neuron survival without expanding the population of either immature or mature neurons.

Lastly, we assessed *Bmp 9* expression in anterior region, posterior region, and hippocampus of wildtype mice. While highly expressed in liver as reported,[5] *Bmp9* expression within the brain was low and comparable to that of hippocampus from *Bmp9*KO mice (Fig. S4). We also quantified neurons expressing choline acetyltransferase (ChaT) and the total number of neurons ($NeuN^+$) in medial septum and diagonal band of Broca (Fig. 1F, *a-d*). Surprisingly, the number of cholinergic neurons did not differ for wildtype and *Bmp9*KO mice (Fig. 1F, *b*), neither did the total number of neurons between wildtype and *Bmp9*KO mice (Fig. 1F, *c*). Similarly, we did not detect any difference in proportion of cholinergic neurons ($ChAT^+$) between the two groups (Fig. 1F, *d*).

Collectively, our work demonstrates that BMP9 modulates mouse adult hippocampal neurogenesis under homeotic condition. Further studies are warranted to determine if BMP9 plays any significant roles in neuronal ageing, neuronal degeneration, and/or acute neuronal damage caused by stroke, ischemic and/or traumatic injuries. Furthermore, it is of significance to investigate if BMP9 play any role in early neurogenesis, as well as potential factors that may functionally compensate BMP9 functions during development.

Conflict of interests

The authors declare no conflict of interest.

Funding

The reported work was supported in part by research grants from the National Institutes of Health (USA)(CA226303 to TCH and DE030480 to RRR). This project was also supported in part by The University of Chicago Cancer Center Support Grant (P30CA014599) and the National Center for Advancing Translational Sciences of the National Institutes of Health (USA) (No. 5UL1TR002389). TCH was also supported by the Mabel Green Myers Research Endowment Fund and The University of Chicago Orthopaedics Alumni Fund (USA). Funding sources were not involved in the study design; in the collection, analysis and interpretation of data; in the writing of the report; and in the decision to submit the paper for publication.

Acknowledgments

MRR wishes to thank Drs. Chip Ferguson, Brian Popko, and Clifton Ragsdale of The University of Chicago, and Dr. Gopal Thinakaran of the University of South Florida for their expert guidance and support during the course of the investigation.

Appendix A. Supplementary data

Supplementary data to this article can be found online at https://doi.org/10.1016/j.gendis.2023.02.018.

References

1. Gage FH. Adult neurogenesis in neurological diseases. *Science*. 2021;374(6571):1049—1050.
2. Mostafa S, Pakvasa M, Coalson E, et al. The wonders of BMP9: from mesenchymal stem cell differentiation, angiogenesis, neurogenesis, tumorigenesis, and metabolism to regenerative medicine. *Genes Dis*. 2019;6(3):201—223.
3. Lopez-Coviella I, Berse B, Krauss R, Thies RS, Blusztajn JK. Induction and maintenance of the neuronal cholinergic phenotype in the central nervous system by BMP-9. *Science*. 2000; 289(5477):313—316.
4. Huang X, Wang F, Zhao C, et al. Dentinogenesis and tooth-alveolar bone complex defects in BMP9/GDF2 knockout mice. *Stem Cell Dev*. 2019;28(10):683—694.
5. Liu W, Deng Z, Zeng Z, et al. Highly expressed BMP9/GDF2 in postnatal mouse liver and lungs may account for its pleiotropic effects on stem cell differentiation, angiogenesis, tumor growth and metabolism. *Genes Dis*. 2020;7(2):235—244.

Mary Rose Rogers [a,b], Wei Zeng [a,c], Xian Zhang [d], Ruidong Li [a,e], Qiang Wei [a,f], Yuhan Kong [a,f], Piao Zhao [a,f], Guozhi Zhao [a,f], Yonghui Wang [a,g], Jiamin Zhong [a,h], Yi Zhu [a,i], Rex C. Haydon [a], Hue H. Luu [a], Russell R. Reid [a,j], Daniel A. Peterson [k], Michael J. Lee [a], Tong-Chuan He [a,b,j,*]

[a] *Molecular Oncology Laboratory, Department of Orthopaedic Surgery and Rehabilitation Medicine, The University of Chicago Medical Center, Chicago, IL 60637, USA*

[b] *Graduate Program Committee on Genetics, Genomics and System Biology, The University of Chicago, Chicago, IL 60637, USA*
[c] *Department of Interventional Neurology, The First Dongguan Affiliated Hospital, Guangdong Medical University, Dongguan, Guangdong 523475, China*
[d] *Department of Neurology, The Second Affiliated Hospital of Jianghan University, Wuhan, Hubei 430000, China*
[e] *Department of Orthopaedic Surgery, The Second Affiliated Hospital of Chongqing Medical University, Chongqing 400010, China*
[f] *Department of Clinical Laboratory Medicine, Rehabilitation Medicine, Orthopaedic Surgery and Urology, The First Affiliated Hospital of Chongqing Medical University, Chongqing 400016, China*
[g] *Department of Endocrinology, Shanghai Jiao-Tong University School of Medicine, Shanghai 200000, China*
[h] *Ministry of Education Key Laboratory of Diagnostic Medicine, and Department of Clinical Biochemistry, The School of Laboratory Medicine, Chongqing Medical University, Chongqing 400016, China*
[i] *Department of Orthopaedic Surgery, Beijing Hospital, Chinese Academy of Medical Sciences & Peking Union Medical College, Beijing 100730, China*
[j] *Laboratory of Craniofacial Suture Biology and Development, Department of Surgery Section of Plastic Surgery, The University of Chicago Medical Center, Chicago, IL 60637, USA*
[k] *Center for Stem Cell and Regenerative Medicine, Rosalind Franklin University of Medicine and Science, North Chicago, IL 60064, USA*

*Corresponding author. Molecular Oncology Laboratory The University of Chicago Medical Center, 5841 South Maryland Avenue, MC3079 Chicago, IL 60637, USA.
E-mail address: tche@uchicago.edu (T.-C. He)

18 December 2022
Available online 29 March 2023